Interference Mitigation for Multi Spot Beam Satellite Communication Systems Incorporating Spread Spectrum

Abdulkareem Karasuwa[1(✉)], Jon Eastment[2], and Ifiok Otung[1]

[1] Mobile and Satellite Communications Research Group,
University of South Wales, Pontypridd CF37 1DL, UK
{abdulkareem.karasuwa,ifiok.otung}@southwales.ac.uk
[2] STFC Rutherford Appleton Laboratory, Harwell Oxford, Didcot OX11 0QX, UK
jon.eastment@stfc.ac.uk

Abstract. Nonlinear precoding techniques have robust transmit power stability and achieve superior interference suppression when compared to their linear counterparts. Tomlinson-Harashima Precoding (THP) is a suboptimal version of Costa's well-known work on writing on dirty paper (DPC). Implementing these precoding techniques in a multi spot beam satellite communications system that employs frequency reuse can significantly reduce co-channel interference (CCI). In this paper, we investigate and compare the performance of linear and nonlinear precoding techniques on the forward link of a multiple spot beam satellite link. In addition, we examine the potential benefits of integrating the novel spread spectrum (SS) technique with the existing precoding techniques. The new system's performance is evaluated and compared with that of standard precoding techniques, and the benefits of incorporating SS are weighed against the extra bandwidth requirements.

Keywords: High throughput satellite · Frequency reuse · Multi spot beam · Co-channel interference · Precoding · Spread spectrum

1 Introduction

The desire to support increasing growth in multimedia applications and services poses a challenge to satellite communication operators to find solutions to the scarcity of bandwidth resources in the legacy frequency bands allocated for satellite services. Options considered include transition to higher frequency bands, such as *Ka* and above, and adoption of advanced signal processing techniques, such as Digital Video Broadcasting second generation (DVB-S2) adaptive modulation and coding (MODCOD), for efficient spectrum utilisation. Systems operating at higher frequencies have to contend with atmospherically-induced propagation perturbations by using fade mitigation techniques [1]. A promising strategy to increase the capacity of satellite systems is the multiple spot beam transmission scheme, which reuses the available spectrum resources, thereby expanding the system's capacity by up to an order of magnitude [2]. This has led to the emergence of so-called high throughput satellite (HTS) systems, deploying large numbers of spot beams (for example, *Ka-Sat* and *ViaSat-1*) [3]. The number of

I. Otung et al. (Eds.): WiSATS 2016, LNICST 186, pp. 156–166, 2017.
DOI: 10.1007/978-3-319-53850-1_16

spot beams and frequency reuse factor (N_{reuse}) dictates the level of co-channel interference (CCI) amongst beams reusing the same colour (i.e. portion of the bandwidth). The highest capacity can be achieved when neighbouring spot beams share the same colour; however, the level of CCI may be severe and can limit system performance [4]. There is, therefore, a compromise between CCI level and system capacity.

Multiple spot beam satellite systems are considered as multiple-input multiple-output (MIMO) systems, with the forward link (for example, gateway via satellite to the user terminal) as a broadcast channel (BC) and the return link (for example, user terminal via satellite to the gateway) as a multiple access channel (MAC) [5]. In order to reduce the impact of CCI in the forward link, precoding can be implemented at the transmitter (gateway or satellite). The benefits of this approach are to relieve the receiver from processing burden, computational complexity and power constraints, leading to simpler, power-efficient and cheaper end-user receivers [6]. On the other hand, for the reverse link, it is well known that multi-user detection (MUDs) techniques, such as successive interference cancellation (SIC), can be used to suppress the effect of CCI [5].

This paper focuses on precoding techniques, which are broadly classified into linear and nonlinear approaches. Linear precoding includes the zero-forcing (ZF) and the minimum mean squared error (MMSE) schemes. They are less complex than nonlinear precoding but offer inferior performance. This is due to the adverse effect of channel matrix inversion, which causes the precoded signal's average energy to exceed that of the original transmitted signal [7]. Alternatively, nonlinear precoding techniques, based on Costa's optimal dirty paper method (DPC) [8], offer superior performance at the expense of extra computational complexity. A simple approach is the Tomlinson-Harashima precoding (THP) [9, 10] which delivers a performance close to that of DPC with moderate computational complexity. An important feature of the nonlinear scheme is that the energy of the precoded signal is approximately the same as that of the original transmitted signal, due to the modulo arithmetic operation introduced by the THP.

The use of linear precoding in the forward link of a broadband multiple spot beam satellite system to curb the effect of CCI has been presented in [11], and shows a significant improvement in system capacity. On the other hand, some popular THP approaches [12, 13] have their implementations extended to multiple spot beam satellite system in [14].

The technical considerations and implications of spread spectrum (SS) techniques over satellite, like multiplexing, coding, and transmission of direct-sequence SS (DS-SS), have been described in detail in [15]. In SS systems, information symbols are encoded using different spreading codes (known as signatures) at the transmitters, the chip-rate of which is significantly higher than that of the information stream. The same bandwidth resource is used by multiple users to simultaneously transmit their SS signals, while the receiver recovers the desired transmitted data by correlating the incoming SS signal with the appropriate user's signature.

In this work, the various implementations of linear and nonlinear precoding are discussed, and an implementation of THP on a multiple spot beam satellite system, based on combining the well-known precoding techniques with SS, is proposed. To the best of our knowledge, the incorporation of SS with THP over multiple spot beam satellite systems is a novel approach. While the method requires increased system complexity and higher bandwidth utilisation, enhanced overall performance is the goal. The performance of the new system is analysed via extensive simulations on a MATLAB platform, and results are compared with the performance of existing methods that are based on precoding alone.

2 The Multiple Spot Beam Satellite Channel

In this case, the satellite antenna feeds (spot beams) represents the transmit antenna elements and the user terminals' antennas can be considered as the elements of the receive antennas of a virtual MIMO system. The MIMO channel, with number of transmit antennas, N_T, and number of receive antennas, N_R, is modelled as [16]:

$$\mathbf{y} = \mathbf{H}\mathbf{b} + \mathbf{n}. \tag{1}$$

where $\mathbf{b}$ is the transmitted signal column vector of size N_T, $\mathbf{b} = \left[b_1, b_2, b_3, \ldots, b_T\right]^T$ each with variance $\mathrm{E}\left\{\left|\mathbf{b}_i\right|^2\right\} = \sigma_b^2$, $\mathbf{y}$ is the received signal symbols column vector of size N_R, $\mathbf{y} = \left[y_1, y_2, y_3, \ldots, y_R\right]^T$, and $\mathbf{n}$ is additive white zero-mean complex noise (AWGN) column vector of size N_R, $\mathbf{n} = \left[n_1, n_2, n_3, \ldots, n_R\right]^T$ with variance $\mathrm{E}\left\{|\mathbf{nn}|^{\mathrm{H}}\right\} = \sigma_n^2\mathbf{I}$. (where $(\cdot)^{\mathrm{T}}$ and $(\cdot)^{\mathrm{H}}$ stand for transpose and conjugate transpose (Hermitian) operations, respectively). The channel matrix $\mathbf{H}$ has dimension N_T by N_R and its h_{ij} elements represents the complex attenuations from the j-th beam to the i-th receiving terminal, with $i = 1, 2, \ldots, N_R$ and $j = 1, 2, \ldots, N_T$. For example, consider the i-th element of $\mathbf{y}$ which is given by:

$$\mathbf{y}_i = \sum_{j=1}^{N_T} h_{ij}\mathbf{b}_j + \mathbf{n}_i. \tag{2}$$

The channel delivers the interfering signal emanating from the spot beams into each of the user terminals via the side-lobe. Note that when $N_T = N_R = N_{SB}$, (N_{SB} is the number of spot beams), $\mathbf{H}$ is an $N_{SB} \times N_{SB}$ invertible square matrix. Therefore,

$$\mathbf{y}_i = h_{ii}\mathbf{b}_i + \sum_{\substack{j=1 \\ j\neq i}}^{N_{SB}} h_{ij}\mathbf{b}_j + \mathbf{n}_i. \tag{3}$$

The wanted user signal is modified by the gain h_{ii}, and distorted by the combined effect of all interference power from co-channel beams which are the off-diagonal elements of $\mathbf{H}$, and the AWGN.

CCI in multiple spot beam systems is influenced by the number of reuse colours, inter-beam spacing and the taper values of the satellite transmit antenna side-lobe levels. The interference decreases with increasing reuse number and decreasing antenna side-lobe level. The total CCI power on the forward link, I_f, in dBW, is given by

$$\sum_{k=1}^{N_{CC}} I_f = EIRP_{SAT} + G_{ES,max} - P_{BO} - L_{ATM} - L_M - L_{FS} + X. \quad (4)$$

Where,

$$X = 10\log_{10} \sum_{k=1}^{N_{CC}} \frac{\left|f_R(\theta_k)^2\right|}{L_S}. \quad (5)$$

In (4) and (5), $EIRP_{SAT}$ is the effective isotropically radiated power of the satellite in dBW, $G_{ES,max}$ is the earth station antenna maximum gain (dBi), P_{BO} is the transmitter power amplifier back-off (dB), L_{ATM} is the atmospheric losses (dB), L_M is the miscellaneous losses (dB), L_S is the antenna scan losses (dB), L_{FS} is the free-space path loss (dB), $f_R(\theta_k)$ is the normalised antenna pattern with taper and N_{CC} is the number of neighbouring co-channel cells.

The forward link of a typical Geostationary (GEO) satellite located at 19.2° East longitude covering Europe with a total of 96 spot beams is used for this analysis, as detailed in [5]. The half-beam width, θ_{3dB} is 0.2°, and a frequency of 20 GHz is used with seven beams ($N_{SB} = 7$) with universal frequency reuse adopted ($N_{reuse} = 1$) so that the six neighbouring co-channel spot beams can contribute maximum interference power possible to the user in the centre of the wanted beam, as indicated in Fig. 1.

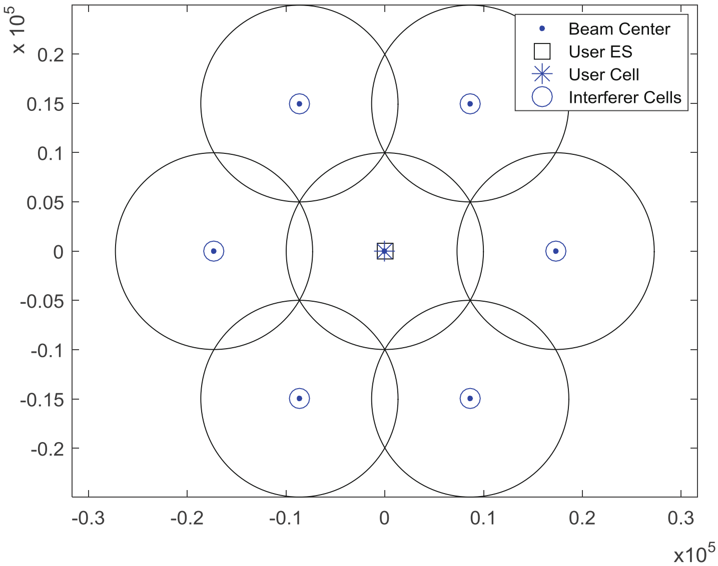

Fig. 1. Location of 7 co-channel beams (each of radius 125 km)

The interferers here are the static co-channel spot beams. Therefore, the distance between each interfering source and the user is the same. This gives rise to the same path loss and off-axis interfering antenna gain towards the user earth station. The antenna pattern, and interferer angular-offset position, is shown in Fig. 2. In addition, this means the phase shift between the beams is constant for each realisation of **H**. The coefficients of **H** and phase shift are obtained using [5]:

$$\mathbf{H} = \left|h_{i,j}\right|\mathbf{\Phi}. \tag{6}$$

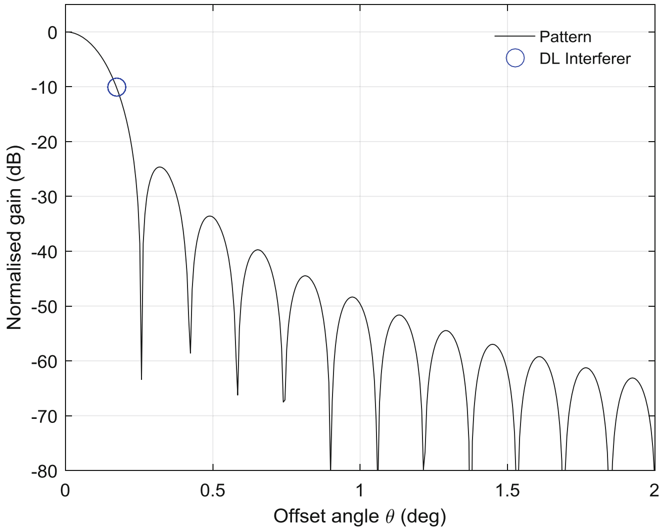

Fig. 2. Normalised satellite antenna gain pattern showing interferer offset angle

Absolute values of the channel coefficients and phase shift are determined by:

$$\left|h_{i,j}\right| = \sqrt{\frac{\mathrm{G}_{i,j}}{\mathrm{L}_{FS,j}} \cdot \frac{\mathrm{L}_{FS,u}}{\mathrm{G}_{ES,max}}}. \tag{7}$$

$$\mathbf{\Phi} = e^{\mathrm{j}\theta_{i,j}}. \tag{8}$$

Where $\mathrm{G}_{i,j}$ is the gain of the interferers towards the user, $\mathrm{L}_{FS,j}$ is the interferers path-loss, $\mathrm{L}_{FS,u}$ is the user path-loss and $\mathrm{G}_{ES,max}$ is the user maximum gain.

3 Linear and Nonlinear Precoding Techniques

In linear precoding, as shown in Fig. 3, the transmit modulated symbols (QPSK or QAM) are multiplied by a precoding matrix **W** and a positive scalar factor β^{-1} at the transmitter. The inverse of β is applied at the receiver in order to meet the total transmitted power constraint after precoding, E_{TX}.

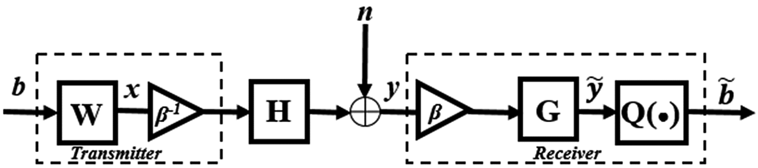

Fig. 3. Block diagram of linear precoding transmitter and receiver

The precoding matrix **W** and its transmit power constraint factor β can be expressed as follows, with subscripts ZF denoting zero-forcing [13]:

$$\mathbf{W}_{ZF} = \frac{1}{\beta}\mathbf{H}^{+} = \frac{1}{\beta}\mathbf{H}^{\mathbf{H}}(\mathbf{H}\mathbf{H}^{\mathbf{H}})^{-1}. \tag{9}$$

$$\beta_{ZF} = \sqrt{\frac{Tr\left(\left(\mathbf{H}\mathbf{H}^{H}\right)^{-1}\sigma_b^2\right)}{E_{TX}}}. \tag{10}$$

where $Tr(\cdot)$ means trace operation and E_{TX} is the transmit energy.

The MMSE precoding matrix $\mathbf{W}_{MMSE}$ and its transmit power constraint factor β_{MMSE} are given by:

$$\mathbf{W}_{MMSE} = \frac{1}{\beta}\left(\mathbf{H}^{H}\mathbf{H} + \xi\mathbf{I}\right)^{-1}\mathbf{H}^{H}. \tag{11}$$

$$\beta_{MMSE} = \sqrt{\frac{Tr\left(\left(\boldsymbol{H}^{H}\boldsymbol{H} + \xi\boldsymbol{I}\right)^{-2}\boldsymbol{H}^{H}\boldsymbol{H}\sigma_b^2\right)}{E_{TX}}}. \tag{12}$$

Where $\xi = N_{SB}\sigma_n^2 / \sigma_b^2$.

The MMSE precoding takes into consideration the noise variance, σ_n^2, to improve performance in the low-SNR region.

The block diagram depicting a THP nonlinear precoding system is shown in Fig. 4.

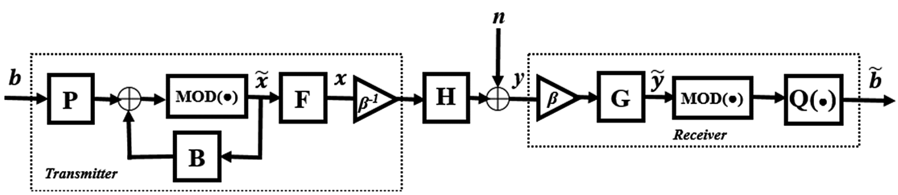

Fig. 4. Block diagram of THP precoding transmitter and receiver

The insertion of the modulo operation into the linear precoding scheme provides the nonlinearity that ensures the amplitude of signal b_i is maintained within the bounds of the original constellation. For *M-QAM* modulation, the modulo operation MOD (·) is defined as [7]:

$$\mathrm{M}(b_i) = b - \left\lfloor \frac{\mathbf{Re}(b_i)}{\tau} + \frac{1}{2} \right\rfloor \tau - j \left\lfloor \frac{\mathbf{Im}(b_i)}{\tau} + \frac{1}{2} \right\rfloor \tau. \tag{13}$$

where τ is a constant for the periodic extension of the constellation, depending on the modulation scheme employed. However, the modulo operation causes a small increase in transmit energy, known as precoding loss, γ_p, which is given by [7]:

$$\gamma_p = \frac{\mathrm{M}}{\mathrm{M} - 1}. \tag{14}$$

In this case, the output of the modulo operation $\tilde{\mathbf{x}}$ is fed into the feed-forward matrix $\mathbf{F}$ yielding the precoded signal $\mathbf{x}$. An extra gain, represented by a diagonal matrix $\mathbf{G}$, is then applied to the rescaled received signal. Finally, the modulo operation is applied to the signal $\tilde{\mathbf{y}}$ and then the estimate $\tilde{\mathbf{b}}$ of the original signal is computed by the decision device Q(•).

4 The Proposed System

The proposed system incorporates spread spectrum with precoding (see Fig. 5). The modulated symbols b_i are precoded as described in Sect. 3. The output x_i of the precoder is then multiplied by a spreading code c_i to yield the spread signal s_i, which is then transmitted via the satellite antenna spot beams and encounters additive white Gaussian noise (AWGN) n_i in the channel. There is no cooperation amongst the user terminals, so each sees only its own channel and is affected by CCI due to side-lobe radiation from co-channel spot beams. The received signal ss_i is de-spread by the dc_i of each receiver yielding xx_i, which is then decoded, reversing the precoding (plus modulo operation – in the case of nonlinear), to give an estimate bb_i of the original transmit symbols.

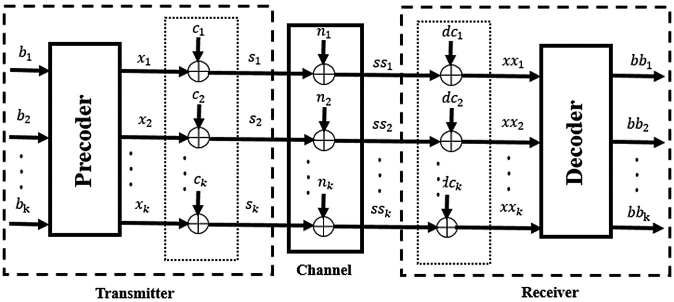

Fig. 5. Block diagram of Precoding plus SS

The advantage of the spreading techniques comes as a processing gain G_p which can be seen as the ratio of the spreading chip's rate R_c over the transmit information rate R_b. This implies the use of significantly wider bandwidth, far more than the usual amount conventionally employed for regular transmission. Higher processing gain also means that lower power is needed for the transmission of information. In essence, bandwidth is traded-off for power - as proposed by Shannon's law. Spreading the information signal with a pseudo-noise (PN) code, which is known to have good auto- and cross-correlation properties [17], can be used to provide interference mitigation. The G_p tends to improve the carrier-to-noise-plus-interference ratio (CNIR) in such a way that will strengthen the diagonal elements and lower the off-diagonal elements of the channel matrix **H**. If we define CNR as the carrier-to-noise ratio, and CIR as the carrier-to-interference ratio, then:

$$\text{CNIR} = \left((\text{CNR})^{-1} + \text{G}_p(\text{CIR})^{-1}\right)^{-1}. \tag{15}$$

$$\text{G}_p = \frac{R_c}{R_b}. \tag{16}$$

With modern HTS systems such as *Hylas* 2 [18] employing transponder bandwidth up to 230 MHz, there is ample scope for SS processing gains in excess of 10 dB to be realised. This translates into significant CCI mitigation that can offset the deficiencies in precoding performance due to an imperfect knowledge of the channel state information (CSI). Therefore, assuming an information bit rate of 40 Mb/s in 20 MHz (QPSK), with this available transponder bandwidth, a chip rate that could offer up to a 7 dB processing gain can be achieved.

5 Results and Discussion

Computer simulations of linear and non-linear precoding were implemented for the satellite system described earlier in this paper. The results shown in Fig. 6 indicate that, where no precoding has been employed, the BER curve exhibits a floor which shows that the system is interference-limited. This is not unexpected, due to the fact that the six neighbouring cells reuse the same frequency spectrum as the wanted user's earth station. It is also clear from the results that the linear precoding techniques improve the system's performance in a manner consistent with the findings of other workers, as reported in the existing literature. The MMSE approach slightly outperformed the ZF approach, with about 1.5 dB additional improvement in the high-SNR region.

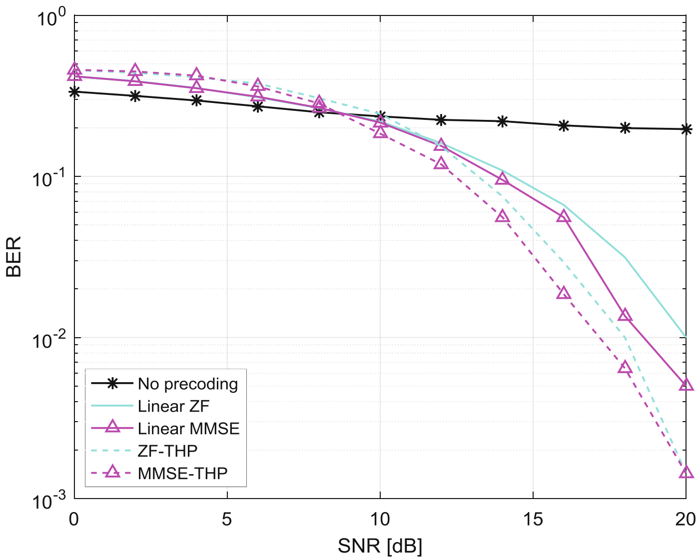

Fig. 6. Comparison of linear and non-linear ZF and MMSE – for QPSK modulation

The non-linear techniques introduce further improvement compared to that offered by the linear approach. The ZF-THP and MMSE-THP are almost 2 dB better than their linear counterparts in the high-SNR region. At lower SNRs, performance of the linear techniques is slightly better than the non-linear techniques; this is, however, not unconnected to the impact of the precoding loss prevalent in the non-linear approach, especially for lower-order modulation schemes like QPSK. This loss is expected to be negligible for higher-order modulation schemes, such as 16-QAM. The no-precoding curve shows better performance at low SNRs, due to the absence of both energy enhancement (for the case of the linear approach) and precoding loss (for the non-linear approach).

Figure 7 shows the results of the impact of the spreading processing gain, G_p on the system performance for the non-linear precoding approach. Due to the reduction of transmit power, there is no significant change in performance between the system with and without spreading for the ZF-THP approach. This is not unconnected with the peculiar effect of the increase in average transmit power, which leads to relatively poor performance. However, for the MMSE-THP approach, the performance improvement due to spreading processing gain is significant. For a BER of 10^{-2}, there is a 4 dB gain in favour of the system that incorporates spread spectrum.

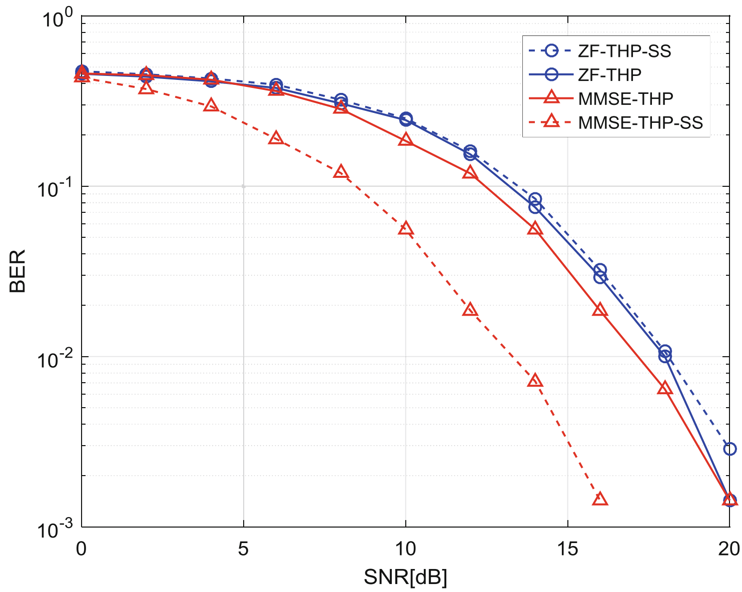

Fig. 7. Comparison of non-linear ZF and MMSE, with and without SS – for QPSK modulation

6 Conclusion

In this work, the impact of co-channel interference on multiple spot beam satellite systems employing extensive frequency reuse has been presented and some methods of mitigating the interference effects have been reviewed and implemented. A new method of improving the performance of precoding techniques has been proposed, and the expected benefits have been discussed. The preliminary results show that incorporating spread spectrum techniques with precoding has the potential to improve interference mitigation performance. It is recognised, however, that this improved performance comes at the expense of both increased complexity and extra bandwidth utilisation. Our future work will concentrate on investigating the system configurations and operational parameters under which the combination of spread spectrum with the various precoding techniques provides maximum scope for improved overall satellite communications system performance.

Acknowledgments. The Authors would like to acknowledge the Petroleum Technology Development Fund (PTDF), Abuja Nigeria which has supported this work.

References

1. Panagopoulos, A.D., Arapoglou, P.M., Cottis, P.G.: Satellite communications at KU, KA, and V bands: propagation impairments and mitigation techniques. IEEE Commun. Surv. Tutorials **6**(3), 2–14 (2004)

2. Lutz, E.: Co-channel interference in high-throughput multibeam satellite systems. In: IEEE International Conference on Communications (ICC) (2015)
3. Lutz, E.: Towards the Terabit/s satellite – interference issues in the user link. Int. J. Satellite Commun. Netw. **34**(4), 461–482 (2015)
4. Karasuwa, A., Eastment, J., Otung, I.: Design considerations for high throughput satellite communication systems. In: 21st Ka and Broadband Communications, Navigation and Earth Observation, Bologna, Italy (2015)
5. Boussemart, V., Berioli, M., Rossetto, F., Joham, M.: On the achievable rates for the return-link of multi-beam satellite systems using successive interference cancellation. In: Military Communications Conference - MILCOM (2011)
6. Joham, M., Utschick, W., Nossek, J.A.: Linear transmit processing in MIMO communications systems. IEEE Trans. Signal Process. **53**(8), 2700–2712 (2005)
7. Fischer, R.F.H.: Precoding and Signal Shaping for Digital Transmission. Wiley, New York (2002)
8. Costa, M.H.M.: Writing on dirty paper (Corresp.). IEEE Trans. Inf. Theory **29**(3), 439–441 (1983)
9. Tomlinson, M.: New automatic equaliser employing modulo arithmetic. Electron. Lett. **7**(5), 138–139 (1971)
10. Harashima, H., Miyakawa, H.: Matched-transmission technique for channels with intersymbol interference. IEEE Trans. Commun. **20**(4), 774–780 (1972)
11. Cottatellucci, L., Debbah, M., Gallinaro, G., Mueller, R., Neiri, M., Rinado, R.: Interference mitigation techniques for broadband satellite systems. In: 24th Proceedings of AIAA International Communication Satellite Systems Conference (ICSSC), San Diego, CA, vol. 1, pp. 1–13 (2006)
12. Fischer, R.F.H., Windpassingre, C., Lampe, A., Huber, J.B.: MIMO precoding for decentralized receivers. In: Proceedings of the IEEE International Symposium on Information Theory (2002)
13. Joham, M., Brehmer, J., Utschick, W.: MMSE approaches to multiuser spatio-temporal Tomlinson-harashima precoding. In: 5th International Conference on Source and Channel Coding (SCC 2004), Erlange, Germany (2004)
14. Diaz, M.A., Courville, N., Mosquera, C., Gianluigi, L., Corazza, G.E.: Non-linear interference mitigation for broadband multimedia satellite systems. In: International Workshop on Satellite and Space Communications (IWSSC 2007) (2007)
15. Gaudenzi, R.D., Giannetti, F., Luise, M.: Advances in satellite CDMA transmission for mobile and personal communications. Proc. IEEE **84**(1), 18–39 (1996)
16. Cho, Y.S., Kim, J., Yang, W.Y., Kang, C.G.: MIMO-OFDM Wireless Communications with MATLAB. Wiley, Singapore (2010)
17. Fazel, K., Kaiser, S.: Multi-carrier Spread Spectrum Systems: From OFDM and MC-CDMA to LTE and WiMAX, 2nd edn. John Wiley and Sons Ltd., Chichester (2008)
18. Avanti Communications Group plc. http://www.avantiplc.com/sites/default/files/hylas-2-tech-sheet.pdf